Electrical transport and electroluminescence properties of n-ZnO single nanowires

INSTITUTE OF PHYSICS PUBLISHING NANOTECHNOLOGY
Nanotechnology **17** (2006) 4868–4872 doi:10.1088/0957-4484/17/19/015

Electrical transport and electroluminescence properties of n-ZnO single nanowires

W Q Yang[1], H B Huo[1], L Dai[1,2,6], R M Ma[1], S F Liu[3], G Z Ran[1,2], B Shen[1,2], C L Lin[4] and G G Qin[1,2,5,6]

[1] School of Physics, Peking University, Beijing 100871, People's Republic of China
[2] State Key Lab for Mesoscopic Physics, Peking University, Beijing 100871, People's Republic of China
[3] HORIBA Yobin Yvon Beijing Representative Office, Beijing 100044, People's Republic of China
[4] Shanghai SIMGUI Technology Co. Ltd, Shanghai 201821, People's Republic of China
[5] Key Lab of Semiconductor Materials, Chinese Academy of Sciences, Beijing 100083, People's Republic of China

E-mail: lundai@pku.edu.cn and qingg@pku.edu.cn

Received 14 June 2006, in final form 10 August 2006
Published 11 September 2006
Online at stacks.iop.org/Nano/17/4868

Abstract
The n-ZnO single nanowire/p^+-Si heterojunctions are fabricated using two types (A and B) of ZnO nanowires. Both types of nanowires are synthesized using the vapour phase transport method. Nanowires A, with growth direction along the high index, are grown on Si substrates. Nanowires B, with growth direction along [0001], are grown on $In_{0.2}Ga_{0.8}N$ substrates. The electrical transport properties of nanowires A and B are investigated by fabricating single nanowire field effect transistors. The measured resistivities are 0.06 and 0.001 Ω cm, respectively. Sharp UV emission resulting from free exciton recombination in ZnO nanowire is observed in the electroluminescence spectra from both types of n-ZnO single nanowire/p^+-Si heterojunctions.

(Some figures in this article are in colour only in the electronic version)

1. Introduction

One-dimensional semiconductor materials have attracted much attention for their potential applications in nano-photonics/electronics. Various kinds of one-dimensional semiconductor nanodevices, such as field-effect transistors (FETs) [1, 2], logic gates [3, 4], and light emitting diodes (LEDs) [5, 6] have been fabricated. Recently, Lieber's group in Harvard University has assembled several kinds of direct band-gap semiconductor nanowires with Si nanowires (NWs) to produce electrically driven nano-photonic systems [7]. This approach has important scientific and technological implications, since a key limitation in Si-based optoelectronics is its very low light emission efficiency due to the indirect band-gap in silicon. ZnO, with its wide direct band-gap (∼3.37 eV) and large room temperature exciton binding energy (60 meV), is a good candidate for ultraviolet (UV) LEDs and lasers [8, 9]. Electroluminescence from ZnO nanowire arrays/p-GaN [10] and ZnO nanowire arrays/p-conducting polymer [11, 12] heterojunctions have been reported recently. However, to our knowledge, electroluminescence from either homojunctions or heterojunctions made from individual ZnO nanowires has not been reported so far. In this paper, we report for the first time on electroluminescence from n-ZnO single nanowire (SNW)/p^+-Si heterojunctions. Two types (A and B) of n-ZnO nanowires were used. Their electrical transport properties were investigated by fabricating single nanowire field effect transistors.

2. Experiments

The ZnO nanowires were synthesized with a commonly used vapour phase transport method. Two types (A and B) of

[6] Authors to whom any correspondence should be addressed.

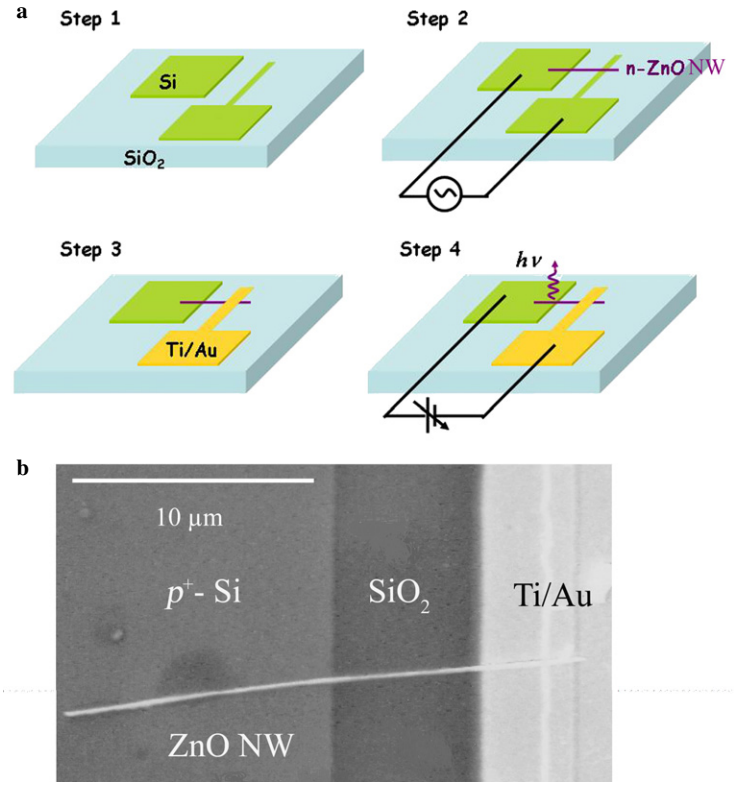

Figure 1. (a) Schematic illustration for the fabrication procedure of n-ZnO SNW/p^+-Si heterojunctions; (b) a FESEM image of an as-fabricated n-ZnO SNW/p^+-Si heterojunction.

substrates were used. Type-A was a p-Si (100) wafer. Type-B was a 50 nm thick $In_{0.2}Ga_{0.8}N$ epilayer grown on sapphire with a GaN buffer layer by metal–organic-chemical-vapour-deposition (MOCVD).

The ZnO nanowires were synthesized in a quartz tube placed in a tube furnace. A layer of thermally evaporated Au film (5–10 nm) on the substrates was used as the catalyst. A mixture of ZnO and graphite powders with a mass ratio of 1:1 was used as the source. The source and the substrates were loaded on a quartz boat, which was then inserted into the quartz tube with the source upstream of high purity N_2 gas. The distance between the source and the substrates was 3–5 cm. The source and substrate temperatures were around 950 and 850 °C, respectively. The growth duration was about 30 min with a high-purity N_2 flow rate of 50 sccm for InGaN substrates and 100 sccm for Si substrates. The as-synthesized products were characterized using a field emission scanning electron microscope (FESEM) (AMRAY 1910 FE) and a high-resolution transmission electron microscope (HRTEM) (Tecnai F30) equipped with an energy-dispersive x-ray (EDX) spectroscope.

The ZnO SNW FETs were fabricated by dropping a ZnO nanowire suspension on oxidized p-Si substrates (with a 600 nm SiO_2 layer on p-Si). The ohmic contacts to source and drain were fabricated by thermally evaporating a Ti/Au (10 nm/120 nm) film on photoresist patterned by UV lithography, followed by a lift-off process. The underlying p-Si substrate was used as the back gate by forming an ohmic contact with an Al electrode. The electrical transport measurements on the ZnO SNW FETs were done by employing a semiconductor parameter characterization system (Keithley 4200). The source electrodes were grounded during the measurements.

The n-ZnO SNW/p^+-Si heterojunctions were fabricated on silicon-on-insulator (SOI) substrates. Each SOI substrate has a 100 nm thick p^+-Si top layer and a 380 nm thick SiO_2 insulator layer. The fabrication procedure is shown in figure 1(a). First, p^+-Si patterns were fabricated by UV lithography and inductively coupled plasma etching. Second, ZnO nanowires were assembled across the edges of the Si patterns to form heterojunctions assisted by AC electric fields [13, 14]. Finally, ohmic contacts to ZnO nanowires were made by the same process as that used in ZnO SNW FETs fabrication. Figure 1(b) shows a FESEM image of an as-fabricated n-ZnO SNW/p^+-Si heterojunction. The electroluminescence spectra from n-ZnO SNW/p^+-Si heterojunctions and the photoluminescence spectra from n-ZnO SNWs were measured using a micro-zone confocal Raman image system (HORIBA Jobin Yvon, LabRam HR800) equipped with a 15× UV lens. A 325 nm He–Cd laser was used as the excitation source.

3. Results and discussion

Figures 2(a) and (d) show FESEM images of the nanowires A and B, respectively. Nanowires A are randomly distributed on Si substrates, while nanowires B are grown vertically from InGaN substrates to form a well-aligned nanowire array. Both nanowires A and B are around 150 nm in diameter and more than 10 μm in length. TEM images of a nanowire A and a

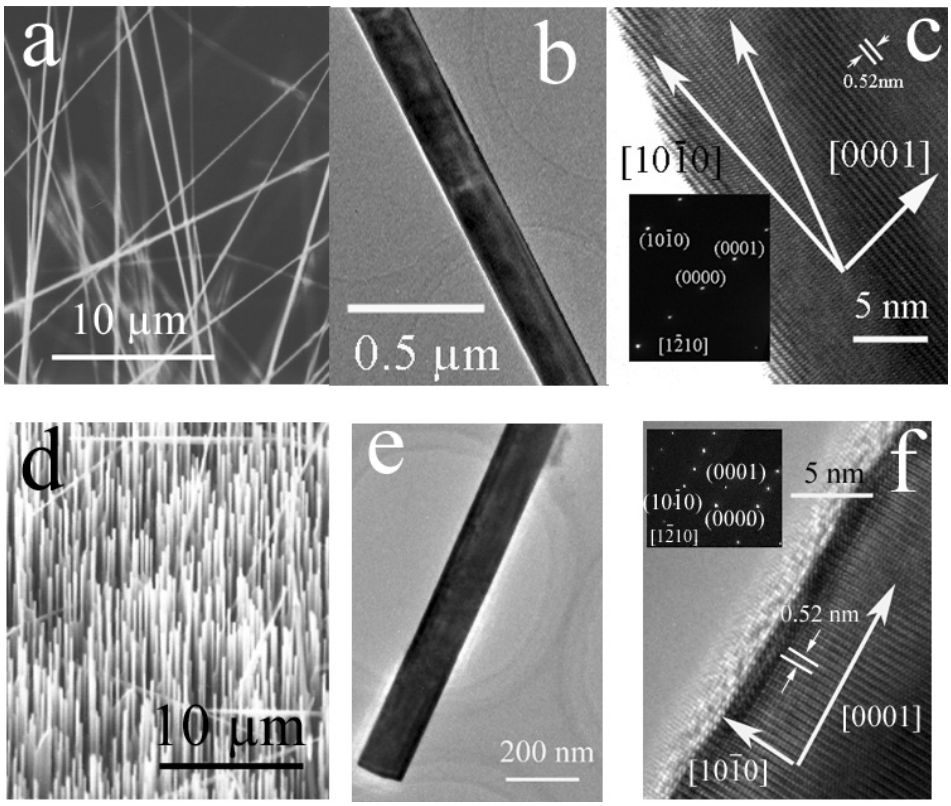

Figure 2. (a) A FESEM image of ZnO nanowires A grown on a Si substrate; (b) a TEM image of a nanowire A; (c) a HRTEM image of the nanowire A depicted in (b). The arrow highlights the growth direction of high index. The inset is the corresponding SAED pattern recorded along the [1$\bar{2}$10] zone axis; (d) a FESEM image of ZnO nanowires B grown on an $In_{0.2}Ga_{0.8}N$ substrate. The well-aligned nanowires form an array; (e) a TEM image of a nanowire B; (f) an HRTEM image of the nanowire B depicted in (e). The arrow highlights the growth direction of [0001]. The inset shows the corresponding SAED pattern recorded along the [12$\bar{1}$0] zone axis.

nanowire B are shown in figures 2(b) and (e), respectively. Both the nanowires A and B have a smooth surface and uniform diameter along the growth direction. Figures 2(c) and (f) are HRTEM images of nanowires A and B, respectively. The insets are the corresponding selected area electron diffraction (SAED) patterns recorded along the [1$\bar{2}$10] zone axis. From these figures, we can see that both nanowires A and B are single crystals with the wurtzite structure. However, nanowires A have a growth direction of high index, which is about 75° away from the [0001] direction, while nanowires B have a growth direction of [0001]. Corresponding Miller indices are labelled in the figures.

The electrical transport measurements on the ZnO SNW FETs made from nanowires A give a linear relation between the source–drain current (I_{sd}) and voltage (V_{sd}), as shown in figure 3(a). This suggests that the Ti/Au electrode has formed a good ohmic contact with nanowire A. The resistivity (ρ) of the nanowires A, as calculated from the I_{sd}–V_{sd} curve in figure 3(a) and dimensions of the nanowire, is about 0.06 Ω cm. Figure 3(b) shows the I_{sd}–V_g curve with $V_{sd} = 3$ V. The source–drain current increases with the gate voltage. This gate-dependence of I_{sd} shows that the conductance type of nanowires A is n-type. Transconductance $g_m (= dI_{sd}/dV_g)$ in the linear region (−32 to 12 V) of figure 3(b) is about 70 nS. Electron mobility (μ) and electron concentration (n) of the nanowires A can be estimated to be about 10 $cm^2\ V^{-1}\ s^{-1}$ and 1×10^{19} cm^{-3}, respectively. The estimation was done using the equations $\mu = g_m \times L \times \ln(2t/r)/(2\pi\varepsilon_0\varepsilon \times V_{sd})$ [2], and $\rho = \frac{1}{en\mu}$, where t and ε are the thickness and the relative dielectric constant of SiO_2, respectively, and r is the radius of the ZnO nanowire.

Figure 3(c) shows the I_{sd}–V_{sd} curve of a SNW FET made from a nanowire B. The calculated ρ is about 0.001 Ω cm. This resistivity is much smaller than that of nanowire A, and is of the same order of magnitude as that of bulk ZnO with electron concentration of 1×10^{19} cm^{-3} and electron mobility of 200 $cm^2\ V^{-1}\ s^{-1}$. No field effect was observed in the SNW FETs made from nanowires B. This indicates that the carrier density in the ZnO nanowire is near the metallic limit [15]. In order to fully understand this, we also grew ZnO nanowires on a GaN substrate with the same synthesis method and fabricated them into SNW FETs. The corresponding electrical transport measurements for these ZnO nanowires gave a resistivity of 0.02 Ω cm, of the same order of magnitude as that of ZnO nanowires grown on Si substrates. This indicates that the high electron concentration in the nanowires B may be due to an n-type doping effect, which may result from diffusion of indium atoms into the ZnO nanowires from the InGaN substrate during the high-temperature synthesis process. We also checked the indium dopants using TEM based EDX. However, no indium element can be detected within the sensitivity limit (∼1%) of the EDX spectroscope.

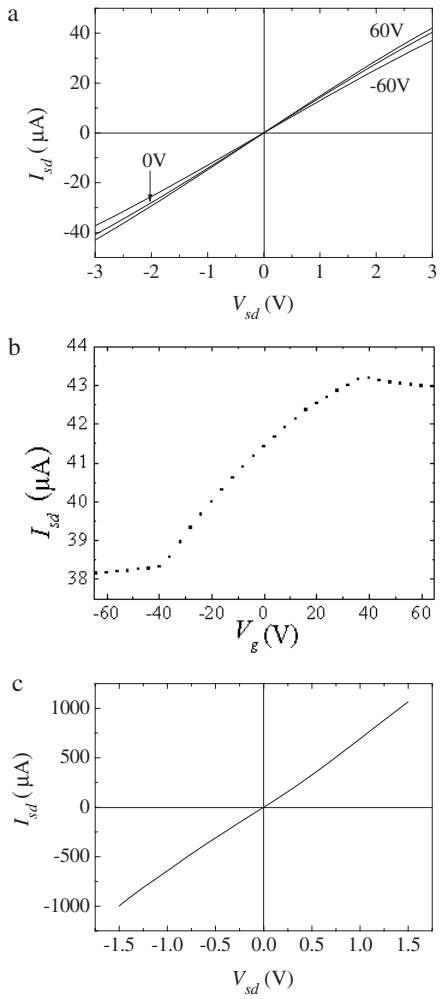

Figure 3. (a) I_{sd}–V_{sd} curves measured on a ZnO SNW A FET, $V_g = -60, 0, 60$ V; (b) I_{sd}–V_g curve measured on the FET, $V_{sd} = 3$ V; (c) a typical I_{sd}–V_{sd} curve for a SNW B FET.

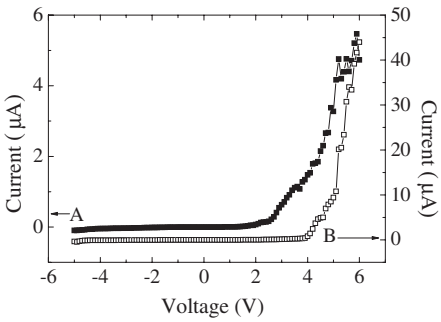

Figure 4. Typical I–V curves of the n-ZnO SNW/p$^+$-Si heterojunctions made from nanowires A and B.

Typical I–V curves of the n-ZnO SNW/p$^+$-Si heterojunctions made from nanowires A and B are shown in figure 4. Both heterojunctions exhibit good rectification characteristics in their I–V curves. The turn-on voltages are 2.5 and 4 V for n-ZnO SNW A/p$^+$-Si and n-ZnO SNW B/p$^+$-Si heterojunctions, respectively.

Figure 5(a) shows the room-temperature electroluminescence spectra from the SNW A/p$^+$-Si heterojunction under various forward biases. A sharp near band-edge emission of the ZnO nanowire with a peak around 382 nm together with a weak broad emission band centred at 700 nm can be found in the electroluminescence spectra when forward bias exceeds 10 V. The full width at half maximum (FWHM) of the ultraviolet (UV) peak is about 13 nm. Figure 5(b) shows the room-temperature electroluminescence spectra from the SNW B/p$^+$-Si heterojunction under various forward biases. At lower forward biases, only a broad emission band centred at 700 nm is observed. When the forward-bias voltage exceeds 8 V, a narrow UV emission around 382 nm appears together with a green emission around 520 nm. The electroluminescence intensities for both heterojunctions increase with forward bias. For comparison, SNW photoluminescence spectra were measured on nanowires A and B, and shown in the inset of figures 5(a) and (b), respectively. For nanowire A, the photoluminescence spectrum is dominated by a sharp UV peak around 382 nm, which results from radiative recombination of free excitons in ZnO [16]. For nanowire B, besides the excitonic emission, a weak broad deep-level defect emission band centred at about 520 nm [17] is observed. We can see that the heterojunction electroluminescence spectra match well with the corresponding ZnO SNW photoluminescence spectra except that there is an additional 700 nm emission band. We think that the 700 nm emission band originates from the luminescence centres located in the native Si oxide layer on the p$^+$-Si substrate, because a very thin native Si oxide layer would form inevitably on the p$^+$-Si in the heterojunction. The 700 nm electroluminescence has been observed and confirmed to result from luminescence centres in the native Si oxide on p$^+$-Si wafers in [18, 19]. The observed higher intensity of the 700 nm electroluminescence band in the ZnO SNW B/p$^+$-Si heterojunction suggests that there may be a thicker Si oxide

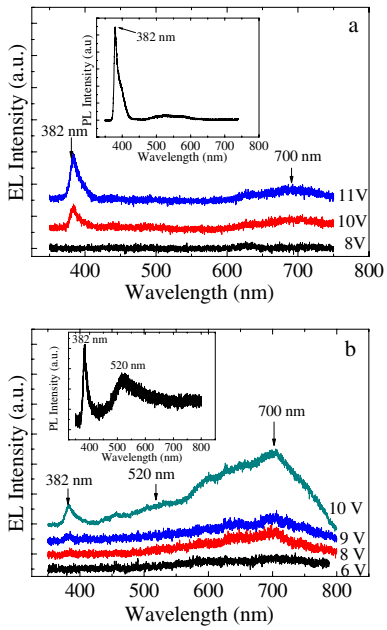

Figure 5. (a) and (b) show room-temperature electroluminescence spectra from n-ZnO SNW A/p$^+$-Si and n-ZnO SNW B/p$^+$-Si heterojunctions, respectively, under various forward biases; the insets in (a) and (b) are photoluminescence spectra from the SNW A and B, respectively.

layer on the p^+-Si used in this heterojunction compared to the ZnO SNW A/p^+-Si heterojunction. This could explain why the turn-on voltage for the ZnO SNW B/p^+-Si heterojunction is higher than that for the ZnO SNW A/p^+-Si heterojunction as shown in figure 4. In our experiment, the injected current densities of the heterojunctions are very low under reverse biases. Therefore we did not observe electroluminescence from ZnO SNW/p^+-Si heterojunctions with reverse biases.

4. Conclusion

In summary, we have fabricated n-ZnO SNW/p^+-Si heterojunctions using two types of ZnO nanowires with different growth directions. Electrical transport measurements on the ZnO SNW FETs show that these ZnO nanowires have low resistivity, which is favourable for making good heterojunctions. Sharp UV emissions resulting from free exciton recombination in ZnO nanowires are observed in the electroluminescence spectra from both types of n-ZnO SNW/p^+-Si heterojunctions. Our results demonstrate a potential application of ZnO nanowires in Si-based nano-optoelectronics.

Acknowledgments

This work was supported by the National Natural Science Foundation of China under grant Nos 10374004, 90201037, 60576037, 10574008, and 50172001, and the National Center for Nanoscience and Technology, China.

References

[1] Cui Y, Zhong Z, Wang D, Wang W U and Lieber C M 2003 *Nano Lett.* **3** 149
[2] Park W, Dim J S, Yi G C, Bae M H and Lee H J 2004 *Appl. Phys. Lett.* **85** 5052
[3] Cui Y and Lieber C M 2001 *Science* **291** 851
[4] Park W, Kim J S, Yi G C and Lee H J 2005 *Adv. Mater.* **17** 1393
[5] Duan X, Huang Y, Cui Y, Wang J and Lieber C M 2001 *Nature* **409** 66
[6] Qian F, Gradecak S, Li Y, Wen C Y and Lieber C M 2005 *Nano Lett.* **5** 2287
[7] Huang Y, Duan X and Lieber C M 2005 *Small* **1** 142
[8] Huang M H, Mao S, Feick H, Yan H, Wu Y, Kind H, Weber E, Russo R and Yang P 2001 *Science* **292** 1897
[9] Tsukazaki A *et al* 2005 *Nat. Mater.* **4** 42
[10] Park W and Yi G C 2004 *Adv. Mater.* **16** 87
[11] Konenkamp R, Word R C and Schlegel C 2004 *Appl. Phys. Lett.* **85** 6004
[12] Konenkamp R, Word R C and Godinez M 2005 *Nano Lett.* **5** 2005
[13] Dong L, Bush J, Chirayos V, Solanki R and Jiao J 2005 *Nano Lett.* **5** 2112
[14] Chen X Q, Saito T, Yamada H and Matsushige K 2001 *Appl. Phys. Lett.* **78** 3714
[15] Cui Y, Duan X F, Hu J T and Lieber C M 2000 *J. Phys. Chem.* B **104** 5213
[16] Kong Y C, Yu D P, Zhang B, Fang W and Feng S Q 2001 *Appl. Phys. Lett.* **78** 407
[17] Vanheusden K, Warren W L, Seager C H, Tallant D K, Voigt J A and Gnade B E 1996 *J. Appl. Phys.* **79** 7983
[18] Qin G G, Huang Y M, Zhang L Z, Zong B Q and Zhang B R 1994 *Superlatt. Microstruct.* **16** 387–90
[19] Qin G G, Huang Y M, Lin J, Zhang L Z, Zong B Q and Zhang B R 1995 *Solid State Commun.* **94** 607–12